

1
2
3
4
5
6
7
8
9
10
11

Optimizing Hydrogen and Ammonia Injection Timing for Enhanced Mixture Formation in Internal Combustion Engines

ABSTRACT

Hydrogen and ammonia are two carbon-free alternative fuels for engines. They represent some of the most viable pathways toward achieving our objectives of energy conservation and reducing emissions. To research the quality of the hydrogen-ammonia-air mixture formation under different hydrogen/ammonia injection timing, a three-dimensional simulation model for a PFI (Port Fuel Injection) hydrogen internal combustion engine with the inlet, outlet, valves and cylinder was established using Converge software. Research focused on the space distribution characteristics and variation law of velocity field, concentration field and turbulent kinetic energy under different injection timings in order to reveal the influence of these parameters on hydrogen-ammonia-air mixture formation process. The results showed that hydrogen injection should be neither too early nor too late. Backfiring can be initiated too early or too late. Therefore, the optimum starting point for hydrogen/ammonia injection should be 338°C.

Keywords: Hydrogen; ammonia; Mixture distribution, injection timing.

1. INTRODUCTION

In recent years, the problem of global warming caused by carbon dioxide emissions from the burning of fossil fuels has attracted considerable attention from all sectors of society, and global carbon dioxide emissions have been increasing year on year, with the burning and use of fossil fuels still accounting for a large proportion of total carbon emissions. Increasingly stringent emission regulations and the national policy direction of green and clean energy consumption have advanced the new trend of green and renewable new energy development, making the development of clean energy occupy an important position in the automotive field[1]. And hydrogen/ammonia has outstanding advantages among many alternative fuels due to its unique physical and chemical properties[2,3]. Hydrogen stands out as the most promising fuel due to its array of favorable characteristics, including its high heating value, rapid flame propagation rate, and notable reaction activity[4,5]. Benbellil conducted experiments on a dual-fuel compression-ignition engine, finding that blending natural gas with hydrogen improved combustion, reduced HC and CO emissions, but cautioned against H₂ concentrations exceeding 50% at high loads due to engine knock[6]. Xin et al. [7] evaluated the combustion and emission performance of the ammonia hydrogen mixed fuel engine. With the hydrogen mixing ratio increasing, the flame propagation speed increasing, the peak of heat release rate increasing, and the ignition timing advance. Frigo investigated the performance impact of burning ammonia/hydrogen dual fuel on a four-stroke gasoline engine, noting that the load primarily influences the ammonia-to-hydrogen ratio, with ignition and combustion rates improving after adding hydrogen, albeit with slightly reduced performance compared to gasoline combustion[8].

12
13
14
15
16
17
18
19
20
21
22
23
24
25
26
27
28
29
30
31
32
33
34
35
36
37
38

39 Wang studied the performance effects of a diesel-fueled ammonia-hydrogen hybrid engine
40 on a high-pressure common rail compression ignition engine, revealing substantial
41 improvements in power and economy with the addition of hydrogen fuel, while noting
42 increased NO_x emissions but significant reduction in N₂O emissions beneficial for global
43 warming mitigation[9].
44 Pure ammonia combustion in engines poses challenges due to high boundary conditions for
45 combustion and prolonged initial flame development[10]. Dimitriou research discovered that
46 achieving pure ammonia combustion is challenging due to its higher ignition temperature
47 compared to diesel, necessitating initial diesel ignition in diesel engines; however, slow
48 flame propagation and high vaporization latent heat values hinder complete combustion,
49 leading to ammonia escape in cases of excessive ammonia blending[11]. Common solutions
50 involve blending combustion with carbon-containing fuels (natural gas, methanol, diesel,
51 gasoline) and hydrogen to lower combustion boundary conditions[12,13]. Sechul investigated
52 a natural gas/ammonia dual-fuel ignition engine, replacing over 50% of natural gas with
53 ammonia fuel, resulting in a more than 28% decrease in CO₂ emissions, alongside a
54 reduction in laminar flame propagation speed as ammonia fuel proportion increased[14].
55 Grannell explored the combustion characteristics of ammonia/gasoline under stoichiometric
56 conditions, and they found that there were no fixed blending ratios between ammonia and
57 gasoline suitable for all operating conditions[15]. Sahin et al. studied the impact of co-
58 combustions an ammonia solution (25% ammonia + 75% water) with diesel fuel on a small
59 diesel engine, finding that while adding ammonia solution to the intake manifold enhanced
60 engine efficiency, it worsened emissions, increasing CO, HC, and NO_x concentrations in the
61 exhaust gas, with only CO₂ emissions decreasing as the ammonia share increased[16].
62 Combining ammonia and hydrogen supply modes offers flexible fuel synergy control
63 strategies to enhance engine performance in internal combustion engines. Rocha
64 numerically examined premixed flame propagation and NO_x emissions in
65 ammonia/hydrogen mixed fuel, finding that while hydrogen addition accelerates flame speed,
66 it significantly increases NO_x emissions[17]. Ichikawa investigated laminar combustion rate
67 and Markstein length in premixed combustion of ammonia-hydrogen mixtures, concluding
68 that using hydrogen as a combustion promoter enhances power and stability, with an optimal
69 hydrogen proportion exceeding 20%[18].
70 In summary, most research on ammonia-hydrogen engines has concentrated on port
71 injection, which, while convenient, reduces volumetric efficiency and power density due to
72 H₂ crowding in the cylinder during the intake stroke. This inspired the present study to
73 investigate the fuel trapping ratio at different injection timings and the velocity and turbulence
74 fields within the cylinder under different injection timings. The research results can promote
75 the practical application of hydrogen fuel in internal combustion engines by providing
76 valuable insights into optimizing combustion processes and enhancing engine efficiency.
77 This could lead to the development of more sustainable and environmentally friendly
78 transportation solutions, contributing to the transition towards cleaner energy sources and
79 reducing carbon emissions in the automotive sector.

80

81

2. COMPUTATIONAL MODEL AND RESEARCH PROGRAM

82

83

2.1 Geometric model

84

85

86

87

88

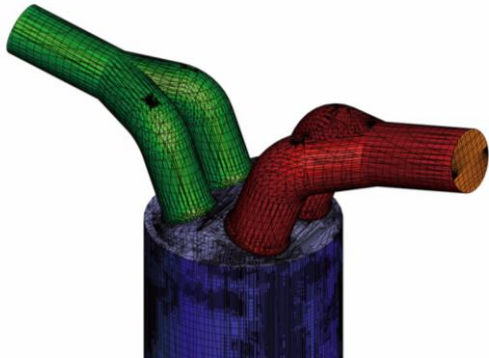
89

90

91

In this paper, a complete closed geometry model consists of inlet and exhaust port, valves and cylinder is established using the three-dimensional modeling software SolidWorks, as shown in Fig. 1(a). The basic parameters of the prototype are shown in Table 1. In order to systematically study the flow and combustion process of the mixture in-cylinder of a PFI hydrogen internal combustion engine, the initial and boundary conditions (including components, temperature, pressure, etc.) were set according to the actual working process of the internal combustion engine with the upper stopping point at the end of the compression stroke as 0 °CA. The base mesh size is 4 mm, with Adaptive Mesh Refinement

92 (AMR) implemented in high-velocity and high-temperature curvature areas. **The engine test**
 93 **bench is shown in Fig. 1 (b).**
 94



95



96

97

98

99

100

101

Fig. 1. (a) 3D Engine Model (b) Engine test bench

Table 1. Parameters of the PFI hydrogen ICE prototype studied in this subject.

Parameters	Indexes
Connecting rod length/mm	160
Cylinder diameter/mm	94
Stroke/mm	85
Compression ratio	9.7:1
Maximum power/kW	30
Maximum power speed/r/min	6000
Maximum torque/N m	51
Maximum torque speed/r/min	4500

102

103

104

105

106

2.2 Numerical model

The CONVERGE software is a computational fluid dynamics software that allows the simulation of combustion, emissions, etc. The main sets of control equations are the mass conservation equation, the momentum conservation equation and the energy conservation

107 equation. In this paper, CONVERGE software is used to establish a 3D simulation model for
 108 simulation research. The sub models used in modeling are as follows:
 109 Turbulence model: The RNG k-ε turbulence model was chosen, which has a high accuracy
 110 of eddy calculation and can better predict the effects of transient flows with a wider range of
 111 applications; Spray model: CONVERGE software accurately models fuel atomization,
 112 evaporation, crushing, and collision using the KH-RT spray fragmentation model, NTC
 113 collision model, and wall film model for droplet-wall interaction; Combustion model: To
 114 ensure the accuracy of the simulation study and better simulate the ignition process and
 115 combustion process in the cylinder, the SAGE combustion model couples the n-
 116 Heptane/hydrogen/ ammonia reaction mechanism in the simulation study.

117 **Mass conservation equation:**

$$118 \quad \frac{\partial \rho}{\partial t} + \frac{\partial \rho u_i}{\partial x_i} = S \quad (1)$$

119 where: t is time; " ρ " is the fluid density; u is the velocity vector; and S is the source term,
 120 originating from evaporation or other submodels.

121 **Equation of conservation of momentum:**

$$122 \quad \frac{\partial \rho u_i}{\partial t} + \frac{\partial \rho u_i u_j}{\partial x_j} = -\frac{\partial P}{\partial x_i} + \frac{\partial \sigma_{ij}}{\partial x_j} + S_i \quad (2)$$

$$123 \quad \sigma_{ij} = \mu \left(\frac{\partial u_i}{\partial x_j} + \frac{\partial u_j}{\partial x_i} \right) + \left(\mu' - \frac{2}{3} \mu \right) \left(\frac{\partial u_k}{\partial x_k} \delta_{ij} \right) \quad (3)$$

124 where: t is time; " ρ " is the fluid density; u is the velocity vector; S is the source term,
 125 originating from evaporation or other sub-models; σ_{ij} is the pressure tensor; P is the
 126 indicated pressure; μ is the viscosity; μ' is the expansion viscosity, which has a value of 0;
 127 and δ_{ij} is the Kronecker function.

128 **Energy conservation equation:**

$$129 \quad \frac{\partial \rho e}{\partial t} + \frac{\partial u_j \rho e}{\partial x_j} = -P \frac{\partial u_j}{\partial x_j} + \sigma_{ij} \frac{\partial u_i}{\partial x_j} + \frac{\partial}{\partial x_j} \left(K \frac{\partial T}{\partial x_j} \right) + \frac{\partial}{\partial x_j} \left(\rho D \sum_m h_m \frac{\rho \gamma_m}{\partial x_j} \right) + S \quad (4)$$

130 where: t is time; " ρ " is the fluid density; u is the velocity vector; S is the source term,
 131 originating from evaporation or other sub-models; T is the temperature; γ_m is the mass
 132 fraction of species m ; D is the mass diffusion coefficient; e is the specific internal energy;
 133 K is the coefficient of transport of matter; and h_m is the enthalpy of species m .

134

135 **2.3 Boundary conditions and initial conditions**

136 In the boundary condition settings for the PFI hydrogen-fueled internal combustion engine,
 137 the air inlet boundary is set to the "inlet" pressure parameter type and the exhaust outlet
 138 boundary to the "outlet" pressure parameter type. In the boundary condition setting of PFI
 139 hydrogen fuel internal combustion engine, the air inlet boundary is set as "inlet" pressure
 140 parameter type, and the exhaust outlet boundary is set as "outlet" pressure parameter type.
 141 The other wall boundaries are set as "fixed wall" with constant temperature; the inlet valve,
 142 exhaust valve and piston are set as "moving wall". Based on preliminary tests and
 143 experience, the following boundary conditions have been established as shown in Table 2.

144

145 **Table 2. Boundary condition setting of PFI hydrogen engine.**

Border areas	Boundary type	Setpoint
Air inlet	Inlet	0.1Mpa
Exhaust outlet	Outlet	0.106Mpa
Inlet pipe	Stationary wall	300K
Exhaustpipe	Stationary wall	600K
Inlet valve	Moving wall	550K
Exhaust valve	Moving wall	800K
Cylinder wall	Stationary wall	480K
Pistons	Moving wall	600K
Cylinder head	Stationary wall	600K

147

148

2.4 Model validation

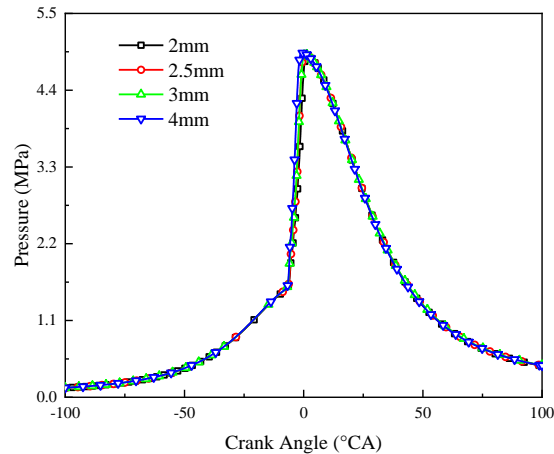
149

150

151

152

Fig. 2 illustrates the impact of base grid size on in-cylinder pressure, showing minor differences when the size is below 4.0 mm, thus justifying a 4 mm base grid size for simulation accuracy and efficiency.



153

154

155

156

Fig.2.The effect of base grid size on in-cylinder pressure.

157

158

159

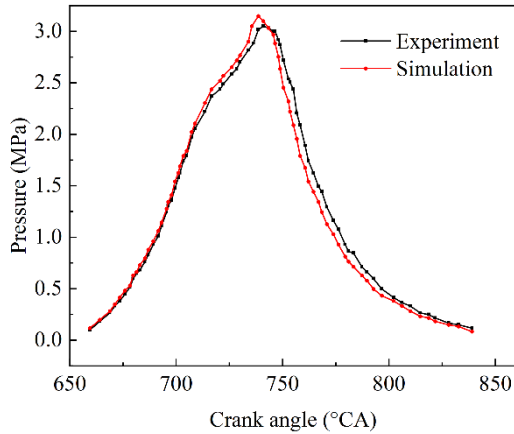
160

161

162

163

Fig. 3 shows the comparison curves of the test and simulated in-cylinder combustion pressures of the hydrogen combustion engine under the same working conditions. It can be seen from Fig. 3 that the experimental and simulation results are in good agreement, and the maximum error is less than 5%. Therefore, it can be proved that the selected hydrogen internal combustion engine model can be used to simulate the in-cylinder combustion process, and the simulation results obtained are highly accurate.



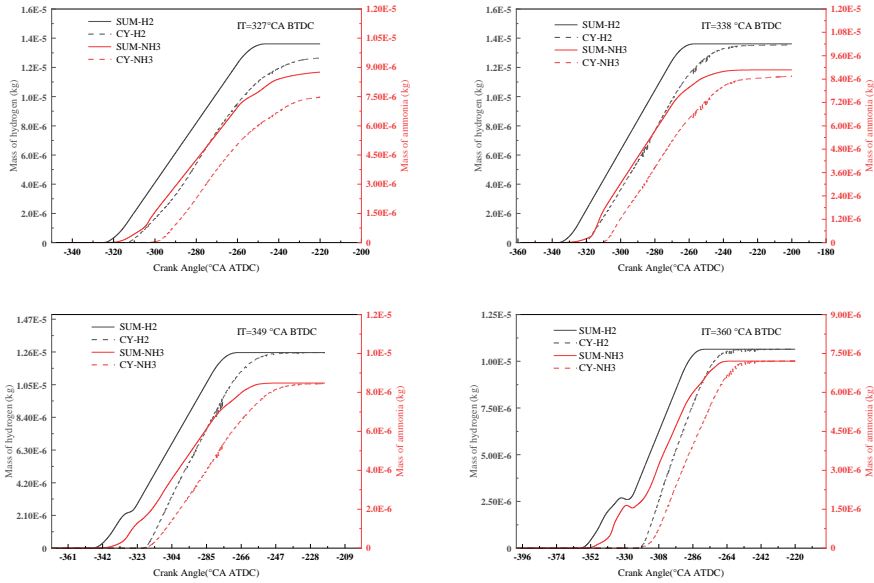
164
165
166 **Fig.3.In-cylinder pressure verification.**

167
168 **2.5 Methodology**

169 The experimental programme with different hydrogen/ammonia injection timing with four sets
170 of hydrogen/ammonia injection timing consists of the following: H338-N338, H338-N349,
171 H349-N338, H349-N349. Where 'H','N' denotes hydrogen/ammonia and '338','349' denotes
172 injection timing of 338° CA BTDC and 349° CA BTDC.

173 An operating cycle of an internal combustion engine consists of four processes: intake,
174 compression, work and exhaust, of which the intake process directly determines the quality
175 of the formation of the mixed fuel and air and has an important influence on the subsequent
176 combustion and emission processes in-cylinder. Hydrogen injection timing is an important
177 factor in controlling the quality of hydrogen-air mixture formation, which directly influences
178 the development and spatial-temporal distribution of hydrogen in the intake tract and into the
179 cylinder, thus essentially inhibiting the problem of intake tract clogging in PFI hydrogen
180 combustion engines. Selecting the optimum timing for hydrogen injection is critical to
181 maximising performance and minimising problems such as intake tract plugging and
182 abnormal combustion. The engine speed is 1800 rpm, the equivalence ratio is 1 and the
183 orifice diameter is 5 mm. Fig. 4 shows the comparison between the set injection volume and
184 the in-cylinder fuel mass at different injection timings with the intake valve closed. From the
185 table, it is learnt that when the injection timing is 338°CA BTDC and 349°CA BTDC, the
186 injection efficiency is the highest and the in-cylinder fuel quality meets the requirements, so
187 the injection timing of 338°CA BTDC and 349°CA BTDC is used as the basis for the next
188 study.

189
190



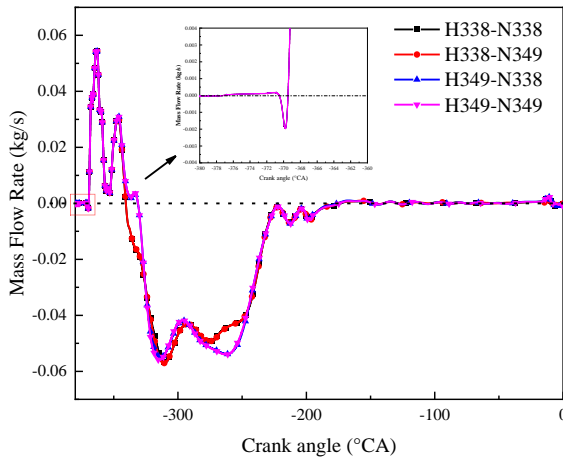
191
192
193
194
195
196
197
198
199
200
201
202
203
204
205
206

Fig.4. In-cylinder fuel capture at different IT.

3. RESULTS AND DISCUSSION

3.1 Effect of injection timing on air flow in the intake pipe

Figure 5 shows the variation of inlet charge mass flow rate with engine crankshaft angle corresponding to five injection timings: H338-N338, H338-N349, H349-N338, H349-N349. In Fig. 5, the vertical coordinate represents the charge inlet mass flow rate, with negative values characterising normal charge flow into the inlet and positive values characterising abnormal charge backflow out of the inlet, representing the occurrence of intake blockage. The increases and decreases described below are based on the zero tick mark, and the increases and decreases are compared in absolute magnitude.



207
208
209
210

Fig.5. Variation of air mass flow with crankshaft under different IT

211 The results in Fig. 5 show that for different injection timing, when the air inlet is opened, the
212 inlet mass flow rate increases slightly in the direction of the inflow inlet and then starts to
213 increase in the direction of the outflow inlet and crosses the zero tick mark, increases rapidly
214 to a peak and then returns to close to the zero tick mark, and then increases again in the
215 direction of the outflow inlet to a peak before returning to the negative range. This is due to
216 the initial period of intake, the valve lift is low, the charge into the intake pipe is hindered,
217 filling the intake pipe after the intake pipe backflow phenomenon occurs, with the gradual
218 opening of the intake valve, the backflow phenomenon is weakened. After the start of the
219 injection timing, due to the small molecular weight of hydrogen, hydrogen is rapidly
220 expanded after being injected into the intake tract, resulting in a rapid increase of the intake
221 mass flow along the outflow direction of the intake tract, and air is rapidly expanded by the
222 hydrogen and forced out of the intake tract, i.e. the air in the intake tract is a backflow
223 phenomenon. This phenomenon is referred to as inlet air blocking phenomenon. At the end
224 of hydrogen injection, there is no more hydrogen expansion and as the piston moves
225 downwards, hydrogen/ammonia is pushed into the cylinder by the air and the air obstruction
226 by hydrogen is reduced and the charge in the intake tract is always in the inflow direction
227 and there is no intake tract backflow. When the hydrogen injection timing was earlier (338°
228 CA BTDC), the intake tract blockage was relieved relatively early, which was more
229 conducive to mixing fuel and air in the cylinder.

230

231 **3.2 Effect of Injection Timing on Velocity Field**

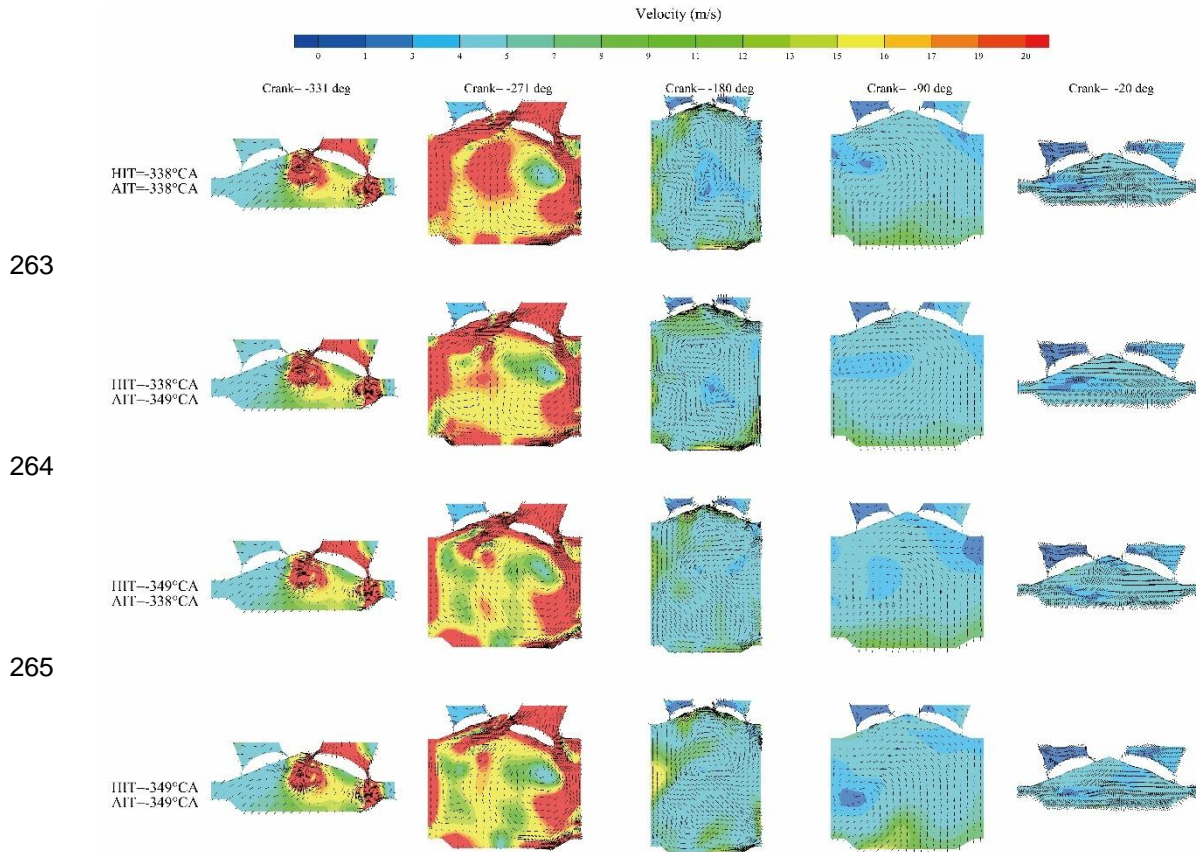
232 Varying the timing of hydrogen injection is of great importance to the law of variation of the
233 in-cylinder velocity field in hydrogen engines. By analysing the velocity field, it is possible to
234 gain insight into the flow characteristics of hydrogen in the combustion chamber, thus
235 optimising the combustion process and improving engine efficiency and performance.

236 As can be seen from the figure, in-cylinder mixture at the beginning of the pressure under
237 the action of the rapid flow to the cylinder. Following an impediment encountered at the
238 intake valve, the amalgamated mixture navigates through a circular conduit between the
239 intake valve and the cylinder head, ultimately coalescing into a localized region of
240 heightened velocity proximal to the intake valve seat. At this juncture, the confined space
241 within the cylinder constrains the voluminous influx, prompting the high-velocity mixture to
242 collide with the cylinder head and piston crown, thereby engendering a pair of counter-
243 rotating vortices under the influence of geometric boundaries.

244 As the intake valve opening continues to increase, the mixture fills the in-cylinder space at a
245 higher flow rate under the effect of injection push and space expansion, and the fuel and air
246 are further mixed. After the piston reaches the lower stop, the in-cylinder space reaches its
247 maximum and the overall flow rate of the mixture slows down. As the compression stroke
248 begins and the piston travels upward, the high flow velocity of the mixture gradually
249 dissipates, with the high flow velocity area existing only at the top of the piston, and the
250 velocity field in other areas being nearly uniformly distributed at an overall velocity. At the
251 moment of ignition, the mixture velocity in-cylinder converges and the velocity field is
252 uniformly distributed.

253 Longitudinal comparison shows that the velocity field of the mixture in the cylinder does not
254 change significantly at the beginning of the intake period, and that, overall, areas of high flow
255 velocity are formed around the valves. Before the piston moves to the lower stop, as the
256 injection timing is delayed, the area of the high-speed area in the cylinder decreases, which
257 is not conducive to rapid mixing of air and fuel; At the beginning of the compression stroke,
258 the high-speed mixture in the cylinder is gradually distributed to the right side of the piston
259 and the left side of the cylinder wall, and the whole tends to be more homogeneous; when
260 the piston moves to the upper stop, the timing of the hydrogen/ammonia injection is all for
261 the -330° CA conditions, with a more uniform distribution of the velocity field.

262



263

264

265

266

267

268

Fig. 6. The development process of the velocity field

269

270

3.3 Effect of Injection Timing on TKE

271

272

273

274

275

276

277

278

279

280

281

282

283

284

285

286

287

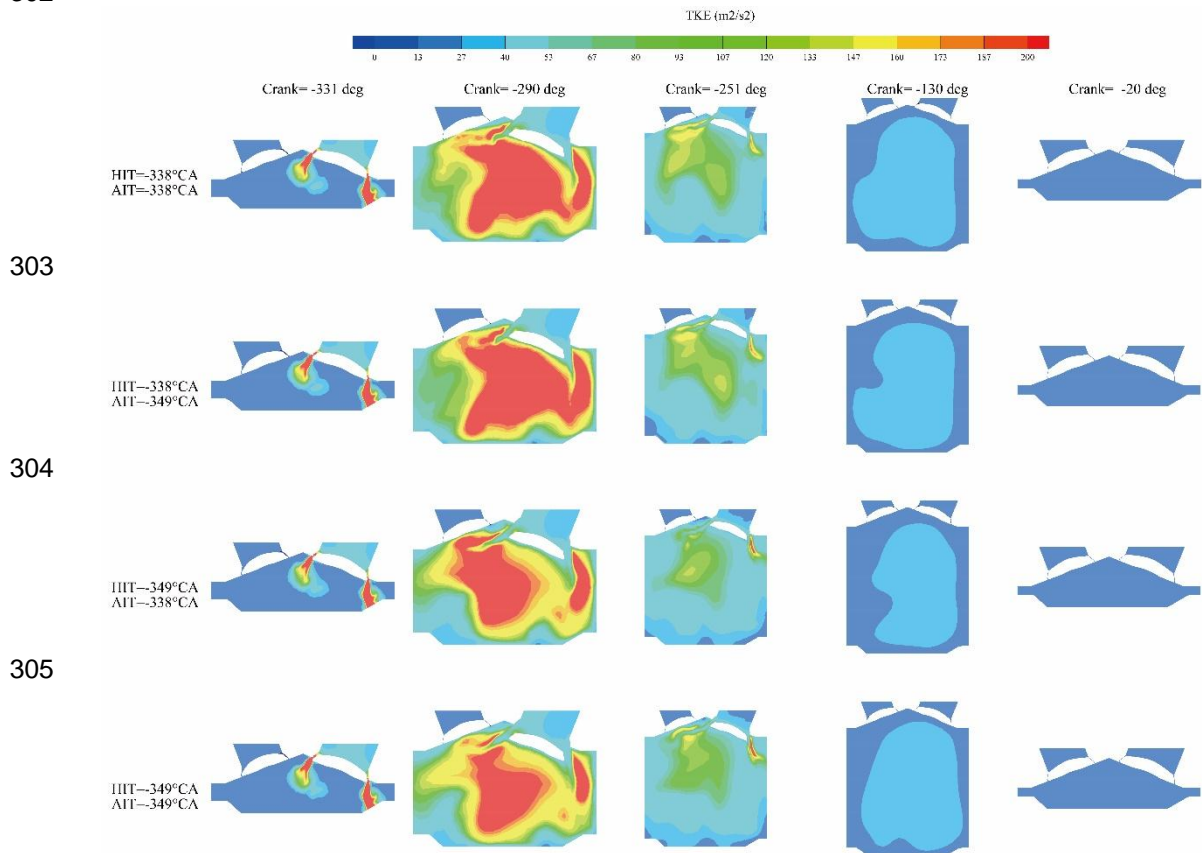
288

289

In practical operation, the port fuel injection (PFI) hydrogen internal combustion engine constantly undergoes a turbulent and highly disordered motion within the confines of its cylinder. Such a phenomenon exerts a discernible influence on the spatio-temporal distribution of various components and the dynamics of both the air-fuel mixture and the flame propagation, thereby exerting a formidable influence on the quality of mixture formation, combustion processes and emission characteristics.

As shown in Fig. 7, at the very beginning of the intake stroke, the high flow rate of the mixture enters the combustion chamber through the valves, and high intensity turbulence is formed around the intake valves, which corresponds to the large scale vortex clusters in the velocity field. As the piston moves down and the intake valve opens, a large amount of gas enters the cylinder along the intake valve and cylinder wall, with higher turbulent kinetic energy at the centre of the cylinder guided by the wall. Towards the end of the inlet stroke, the high turbulent kinetic energy mixture dissipates into low-intensity turbulence, thus favouring homogeneous mixing of the mixture. During the compression stroke, the turbulent kinetic energy enhanced by the compression stress and the shear force between the gas and the wall is not enough to compensate for the rapid dissipation of the turbulent vortices. At this point, the average turbulent kinetic energy in-cylinder continues to decrease. With the upward movement of the piston, the large-scale turbulent vortices continue to break up into small-scale turbulent vortices, and the turbulent motion in-cylinder gradually develops to be

290 dominated by the small-scale turbulent vortices, and the turbulent kinetic energy can be
 291 enhanced accordingly.
 292 A comprehensive comparison shows that the initial high turbulence kinetic energy area is
 293 larger when the injection timing is advanced. The advance in injection timing results in the
 294 mixture entering the cylinder earlier, which encourages a more even distribution of the
 295 mixture in-cylinder. This advance in injection results in better mixing of the mixed fuel with
 296 the air in-cylinder, ensuring that the fuel and oxygen are in full contact to form a more
 297 homogeneous mixture. As a result, at the moment of ignition, the fuel can be burned more
 298 quickly and fully, thus improving combustion efficiency and combustion performance. In
 299 addition, injection timing advance also helps to reduce the stagnation time of the mixture in-
 300 cylinder, reducing incomplete combustion and emissions.
 301
 302



303

304

305

306

307

308

309

310

311

312

313

314

315

316

317

318

Fig. 7. Changes of turbulent kinetic energy in the cylinder

4. CONCLUSION

By studying the spatial distribution characteristics and change laws of total hydrogen quality inside and outside the cylinder, velocity field and turbulent kinetic energy of hydrogen internal combustion engine under different injection timings in the intake pipe, the influence of these parameters on the hydrogen-ammonia-air mixture formation process is revealed. The main findings are shown below.

To improve the uniformity of the gas mixture, the hydrogen injection should be neither too early nor too late. the relative residence time of the high concentration gas mixture in the

319 intake is longer if the injection is too early, which easily leads to backfire. If the hydrogen
320 injection is late, the increase in cylinder pressure hinders the process of the hydrogen
321 entering the cylinder. This also increases the dwell time of the hydrogen at the intake valve.
322 At this point, the mixture will be less uniform. If the hydrogen injection is delayed, the
323 residual hydrogen in the intake pipe can also increase, which increases the possibility of
324 backfire. Therefore, in a comprehensive consideration, the optimum starting point for
325 hydrogen/ammonia injection should be 338°CA.
326 Future areas of research will include further optimisation of injection timing, considering
327 sequential hydrogen/ammonia injection or multiple injection.

328 **ACKNOWLEDGEMENTS**

329

330 Funding: This work is supported by the Project of Educational Commission of Henan
331 Province of China (No. 23A470012).

332

333 **COMPETING INTERESTS**

334

335 The authors declare that they have no known competing financial interests or personal
336 relationships that could have appeared to influence the work reported in this paper.

337

338 **AUTHORS' CONTRIBUTIONS**

339

340 **Shuman Guo**: Conceptualization, Methodology, Validation, Formal analysis, Writing-original
341 draft, Writing – review & editing. **Zhichao Lou**: Software, Investigation, Formal analysis,
342 Writing - original draft. **Xu Zhang**: Software, Formal analysis. **Shaokai Shen**: Investigation,
343 Software, Formal analysis. **Jintao Meng**: Data curation. **Jiaqi Wang**: Data curation. **Chunjian**
344 **Zhou**: curation.

345

346 **REFERENCES**

347

- 348 1. Shang W, Yu X, Shi W, Chen Z, Liu H, Yu H, et al. An Experimental Study on
349 Combustion and Cycle-by-Cycle Variations of an N-Butanol Engine with Hydrogen Direct
350 Injection under Lean Burn Conditions. *Sensors* 2022;22:1229.
351 <https://doi.org/10.3390/s22031229>.
- 352 2. Ishii T, Yamada K, Osuga N, Imashiro Y, Ozaki J. Single-Step Synthesis of W2C
353 Nanoparticle-Dispersed Carbon Electrocatalysts for Hydrogen Evolution Reactions
354 Utilizing Phosphate Groups on Carbon Edge Sites. *ACS Omega* 2016;1:689–95.
355 <https://doi.org/10.1021/acsomega.6b00179>.
- 356 3. Thermo - environomic evaluation of the ammonia production - Tock - 2015 - The
357 Canadian Journal of Chemical Engineering - Wiley Online Library n.d.
358 <https://onlinelibrary.wiley.com/doi/abs/10.1002/cjce.22126> (accessed March 14, 2024).
- 359 4. Gao J, Zhang H, Li J, Wang Y, Tian G, Ma C, et al. Simulation on the effect of
360 compression ratios on the performance of a hydrogen fueled opposed rotary piston
361 engine. *Renew Energy* 2022;187:428–39. <https://doi.org/10.1016/j.renene.2022.01.091>.
- 362 5. Nag S, Dhar A, Gupta A. Hydrogen-diesel co-combustion characteristics, vibro-acoustics
363 and unregulated emissions in EGR assisted dual fuel engine. *Fuel* 2022;307:121925.
364 <https://doi.org/10.1016/j.fuel.2021.121925>.
- 365 6. Benbellil MA, Lounici MS, Loubar K, Tazerout M. Investigation of natural gas enrichment
366 with high hydrogen participation in dual fuel diesel engine. *Energy* 2022;243:122746.
367 <https://doi.org/10.1016/j.energy.2021.122746>.
- 368 7. Xin G, Ji C, Wang S, Meng H, Chang K, Yang J. Effect of different volume fractions of
369 ammonia on the combustion and emission characteristics of the hydrogen-fueled

- 370 engine. Int J Hydrog Energy 2022;47:16297–308.
371 <https://doi.org/10.1016/j.ijhydene.2022.03.103>.
- 372 8. Frigo S, Gentili R. Analysis of the behaviour of a 4-stroke Si engine fuelled with ammoni
373 a and hydrogen. Int J Hydrog Energy 2013;38:1607–15. <https://doi.org/10.1016/j.ijhydene.2012.10.114>.
374
- 375 9. Wang B, Yang C, Wang H, Hu D, Wang Y. Effect of Diesel-Ignited Ammonia/Hydrogen
376 mixture fuel combustion on engine combustion and emission performance. Fuel
377 2023;331:125865. <https://doi.org/10.1016/j.fuel.2022.125865>.
- 378 10. Zhang R, Chen L, Wei H, Li J, Chen R, Pan J. Understanding the difference in
379 combustion and flame propagation characteristics between ammonia and methane
380 using an optical SI engine. Fuel 2022;324:124794.
381 <https://doi.org/10.1016/j.fuel.2022.124794>.
- 382 11. Dimitriou P, Javaid R. A review of ammonia as a compression ignition engine fuel. Int J
383 Hydrog Energy 2020;45:7098–118. <https://doi.org/10.1016/j.ijhydene.2019.12.209>.
- 384 12. Chen J, Jiang X, Qin X, Huang Z. Effect of hydrogen blending on the high temperature
385 auto-ignition of ammonia at elevated pressure. Fuel 2021;287:119563.
386 <https://doi.org/10.1016/j.fuel.2020.119563>.
- 387 13. Zhu X, Khateeb AA, Guiberti TF, Roberts WL. NO and OH* emission characteristics of
388 very-lean to stoichiometric ammonia–hydrogen–air swirl flames. Proc Combust Inst
389 2021;38:5155–62. <https://doi.org/10.1016/j.proci.2020.06.275>.
- 390 14. Oh S, Park C, Kim S, Kim Y, Choi Y, Kim C. Natural gas–ammonia dual-fuel combustion
391 in spark-ignited engine with various air–fuel ratios and split ratios of ammonia under part
392 load condition. Fuel 2021;290:120095. <https://doi.org/10.1016/j.fuel.2020.120095>.
- 393 15. Grannell SM, Assanis DN, Gillespie DE, Bohac SV. Exhaust Emissions From a
394 Stoichiometric, Ammonia and Gasoline Dual Fueled Spark Ignition Engine, American
395 Society of Mechanical Engineers Digital Collection; 2009, p. 135–41.
396 <https://doi.org/10.1115/ICES2009-76131>.
- 397 16. Şahin Z, Ziya Akcanca İ, Durgun O. Experimental investigation of the effects of ammonia
398 solution (NH₃OH) on engine performance and exhaust emissions of a small diesel
399 engine. Fuel 2018;214:330–41. <https://doi.org/10.1016/j.fuel.2017.10.034>.
- 400 17. da Rocha RC, Costa M, Bai X-S. Chemical kinetic modelling of ammonia/hydrogen/air
401 ignition, premixed flame propagation and NO emission. Fuel 2019;246:24–33.
402 <https://doi.org/10.1016/j.fuel.2019.02.102>.
- 403 18. Ichikawa A, Hayakawa A, Kitagawa Y, Kunkuma Amila Somarathne KD, Kudo T,
404 Kobayashi H. Laminar burning velocity and Markstein length of ammonia/hydrogen/air
405 premixed flames at elevated pressures. Int J Hydrog Energy 2015;40:9570–8.
406 <https://doi.org/10.1016/j.ijhydene.2015.04.024>.
- 407 19. Tan D, Meng Y, Tian J, Zhang C, Zhang Z, Yang G, et al. Utilization of renewable and
408 sustainable diesel/methanol/n-butanol (DMB) blends for reducing the engine emissions
409 in a diesel engine with different pre-injection strategies. Energy 2023;269:126785.
410 <https://doi.org/10.1016/j.energy.2023.126785>.
411